



## **Deliverable D2.10:**

**HLW: Report describing the selected experiments  
and the existing/expected experimental results**

Work Package [ACED](#)

The project leading to this application has received funding from the European Union's Horizon 2020 research and innovation programme under grant agreement No 847593.



**EURAD** Deliverable D2.10 – HLW: Report describing the selected experiments and the existing / expected experimental results

#### Document information

Project Acronym	<b>EURAD</b>
Project Title	<b>European Joint Programme on Radioactive Waste Management</b>
Project Type	<b>European Joint Programme (EJP)</b>
EC grant agreement No.	<b>847593</b>
Project starting / end date	<b>1<sup>st</sup> June 2019 – 30 May 2024</b>
Work Package No.	<b>WP2</b>
Work Package Title	<b>Assessment of Chemical Evolution of ILW and HLW Disposal Cells</b>
Work Package Acronym	<b>ACED</b>
Deliverable No.	<b>1</b>
Deliverable Title	<b>HLW: Report describing the selected experiments and the existing/expected experimental results</b>
Lead Beneficiary	<b>MTA EK</b>
Contractual Delivery Date	<b>December 2019</b>
Actual Delivery Date	<b>September 2020</b>
Type	<b>Report</b>
Dissemination level	<b>PU</b>
Authors	<b>Stéphane Gin (CEA), Florent Tocino (EDF), Karine Ferrand (SCK-CEN), Christelle Martin (Andra), Margit Fabian (MTA EK)</b>

#### To be cited as:

Gin, S., Tocino, F., Ferrand, K., Martin, C., Fabian, M. (2019): HLW: Report describing the selected experiments and the existing/expected experimental results. Final version as of 17/12/2019 of deliverable D2.10 of the HORIZON 2020 project EURAD. EC Grant agreement no: 847593.

#### Disclaimer

All information in this document is provided "as is" and no guarantee or warranty is given that the information is fit for any particular purpose. The user, therefore, uses the information at its sole risk and liability. For the avoidance of all doubts, the European Commission has no liability in respect of this document, which is merely representing the authors' view.

#### Acknowledgement

This document is a deliverable of the European Joint Programme on Radioactive Waste Management (EURAD). EURAD has received funding from the European Union's Horizon 2020 research and innovation programme under grant agreement No 847593.

**EURAD** Deliverable D2.10 – HLW: Report describing the selected experiments and the existing / expected experimental results

<b>Status of deliverable</b>		
	<b>By</b>	<b>Date</b>
Delivered (Lead Beneficiary)	Fabian Margit	27 November 2019
Verified (WP Leader)	Diederik Jacques	17 December 2019
Reviewed (Reviewers)	SCK CEN	14 January 2020
Approved (PMO)	Laurent TRENTY on behalf of the PMO	26 May 2020
Submitted to EC (Coordinator)	Andra	28 September 2020

## Executive Summary

The main objective of the EURAD project ACED (Assessment of Chemical Evolution of ILW and HLW Disposal Cells) is to improve methodologies to obtain multi-scale quantitative models for the description of the chemical evolution at the disposal cell scale and to derive robust mathematical models including the most relevant processes.

For the interface and waste package scale, existing data on materials and material interfaces are combined with data from currently running experiments and few complementary new experimental set-ups for evaluating the process integration methodology. While on interface scale investigations concentrate on steel-cementitious and steel-clay interfaces, on waste package scale long-term concrete degradation and implications of waste degradation are the focus.

The subtask 3.1 concerns the first upscaling step from the relatively isolated processes at interfaces to repository sub-systems, representative for HL waste packages, where chemical and physical processes might be closely intertwined.

In case of HLW waste and according to existing HLW concepts in Europe, the subtask 3.1 concentrates on the study of three experimental systems: « Glass/steel/clay » to « Glass/steel/cement » with an intermediate case « Glass/steel/cement buffer/clay »

These systems allow to studying the different interfaces expected in HLW disposal cells with vitrified waste, metallic components, presence of cementitious material and near-field host rock.

This deliverable gives a first overview of information already available about existing or currently running experiments:

Glass/Steel/Clay experiment performed by CEA and running for 5 years at 50°C (§. 2),

Glass/Steel/Cement-bentonite/Clay experiment at 70°C by EDF and launched in April 2018 (§. 3),

Glass/Steel/Cement experiment carried out by SCK-CEN on 20-25°C between 2009 and 2013 (§. 4).

The different modelling approach will begin with the experimental data already available at the beginning of ACED and presented in this deliverable. The modelling work of a HLW waste package and disposal cell will be shared between subtask 3.2 and Task 4.

## Table of content

Executive Summary.....	4
Table of content.....	5
List of figures .....	6
List of Tables .....	7
Glossary.....	8
1. Introduction .....	9
2. Experiment 1: Glass/Steel/Clay system, 50°C .....	12
3. Experiment 2: Glass/Steel/Cement-bentonite/Clay system, 70°C .....	17
4. Experiment 3: Glass/Steel/Cement system, 25°C.....	22
5. Concluding remarks.....	32
6. References .....	33

## List of figures

Figure 1-1 – Overall scope of the project, together with the link to (sub)task and information exchange between tasks.....	9
Figure 1-2 – Interfaces of interest for HLW disposal.....	10
Figure 2-1 – Experimental setup .....	12
<i>Figure 2-2 – Global view of the glass/steel interface. GAL stands for glass altered layer.....</i>	<i>14</i>
<i>Figure 2-3 – Glass alteration layer determined by SEM-EDX.....</i>	<i>14</i>
<i>Figure 2-4 – Si and Fe behavior based on ToF-SIMS mapping.....</i>	<i>15</i>
<i>Figure 2-5 – Secondary phases identified by TEM.....</i>	<i>15</i>
Figure 3-1 – Stainless steel reactors.....	17
Figure 3-2 – Stainless steel reactor schematic representation.....	18
Figure 3-3 – AVM glass sample monolith facing steel after being dissolved for 6 months.....	20
Figure 3-4 – Alteration layer thickness measured on AVM glass after 6 and 12 months.....	21
Figure 3-5 – Alteration layer thickness measured on AVM (with buffer) glass after 6 and 12 months.....	21
Figure 4-1 – Experimental set-up for the integrated tests.....	22
Figure 4-2 – SEM micrograph of lamellar layers observed on SM539 glass particles close to the filter.....	27
Figure 4-3 – SEM micrograph of the cement plug close to the stainless steel filter in the test with SM539 glass. The filter is situated at the right hand side of the micrograph.....	28
Figure 4-4 – SEM micrographs of a spherical hole filled with ettringite and portlandite, and of a non-spherical hole in the cement plug.....	28
Figure 4-5 – SEM micrograph and EDX elemental mappings of the stainless steel filter close to the cement plug in the test with SON68 glass.....	29

## List of Tables

Table 2-1 – Initial composition of the leaching solution.....	13
Table 3-1 –Configurations tested .....	18
Table 3-2 –Schedule .....	18
Table 3-3 –Mass of reagents for 1 kg of solution .....	19
Table 4-1 –Experimental conditions for the integrated tests (uncertainties are given at $2 \sigma$ (95 % confidence interval)). .....	23
Table 4-2 –Duration in days between the start of the tests (i.e. the percolation date) and the sampling dates. ....	23
Table 4-3 - Glass dissolution rates in $g.m^{-2}.d^{-1}$ determined from different leaching tests in YCWCa; the uncertainty at 2 sigma (95% confidence interval is <15%).....	24
Table 4-4 –Average analytical composition in weight % of C42.5 HSR5R LA CCB Portland cement provided by Cibelcor (3 wt% of tricalcium aluminate (C3A) is also reported). ....	25
Table 4-5 –Composition of SON68 and SM539 HE 540-12 glasses in weight %.....	26
Table 4-6 –Composition of the Young Cement Water with Ca (YCWCa) in mg/L. ....	26

## Glossary

ACED	Assessment of Chemical Evolution of ILW and HLW Disposal Cells
AVM	Atelier de Vitrification de Marcoule (Marcoule vitrification facility)
C-A-S-H	Calcium Alumina Silicate Hydrate
CIGEO	Centre Industriel de stockage GEOlogique
COx	Callovo-Oxfordian
C-S-H	Calcium Silicate Hydrate
GAL	Glass Alteration Layer
HLW	High Level Waste
HRTEM	High-Resolution Transmission Electron Microscopy
ICP	Iron Corrosion Products
ICP-AES	Inductively Coupled Plasma – Atomic Emission Spectrometry
ICP-MS	Inductively Coupled Plasma – Mass Spectroscopy
ILW	Intermediate Level Waste
LIBS	Laser Induced Breakdown Spectroscopy
PG	Pristine Glass
URL	Underground Research Laboratory
SEM	Scanning Electron Microscopy
SEM EDX	Scanning Electron Microscopy with Energy Dispersive X-ray analysis
STXM	Scanning Transmission X-ray Microscopy
TEM	Transmission Electron Microscopy
ToF-SIM	Time of Flight Secondary Ion Mass Spectrometry
YCWCa	Young Cementitious Water at pH 13.5

## 1. Introduction

The broader scope of the work package ACED is the assessment of the chemical evolution at the disposal cell scale involving interacting components/materials and thermal, hydraulic and/or chemical gradients by considering ILW and HLW disposal concepts representative for different concepts throughout Europe. To increase the attention towards relevant materials and processes, the work package addresses ILW and HLW components up to the disposal cell scale. The study of the disposal cell in this WP ranges from microscale processes at interfaces between different materials up to interactions of waste packages with their immediate surrounding near field environment and the host rock.

The main objective is to improve methodologies to obtain multi-scale quantitative models for the chemical evolution at the disposal cell scale based on existing and new experimental data and process knowledge and to improve the description of the most relevant processes driving the chemical evolution into robust mathematical frameworks.

More specifically, ACED (*Figure 1-1*) seeks to:

- Compile and integrate the process level knowledge and description of reactivity at the interfaces between materials relevant for ILW and HLW disposal cells
- Develop and evaluate methodologies to integrate available process-level knowledge and processes into a multi-process and multi-scale modelling framework for assessing chemical evolution at the disposal cell level
- Propose and apply a step-wise scale-up process-based approach to identify (i) processes and features which control the chemical evolution for representative HLW and ILW disposal cells and (ii) to which detail and complexity these processes should be incorporated in models for different type of safety and performance related studies. The information gained through study of the more generic but European representative HLW and ILW disposal cells can later be used and adapted for more specific national disposal cell designs.

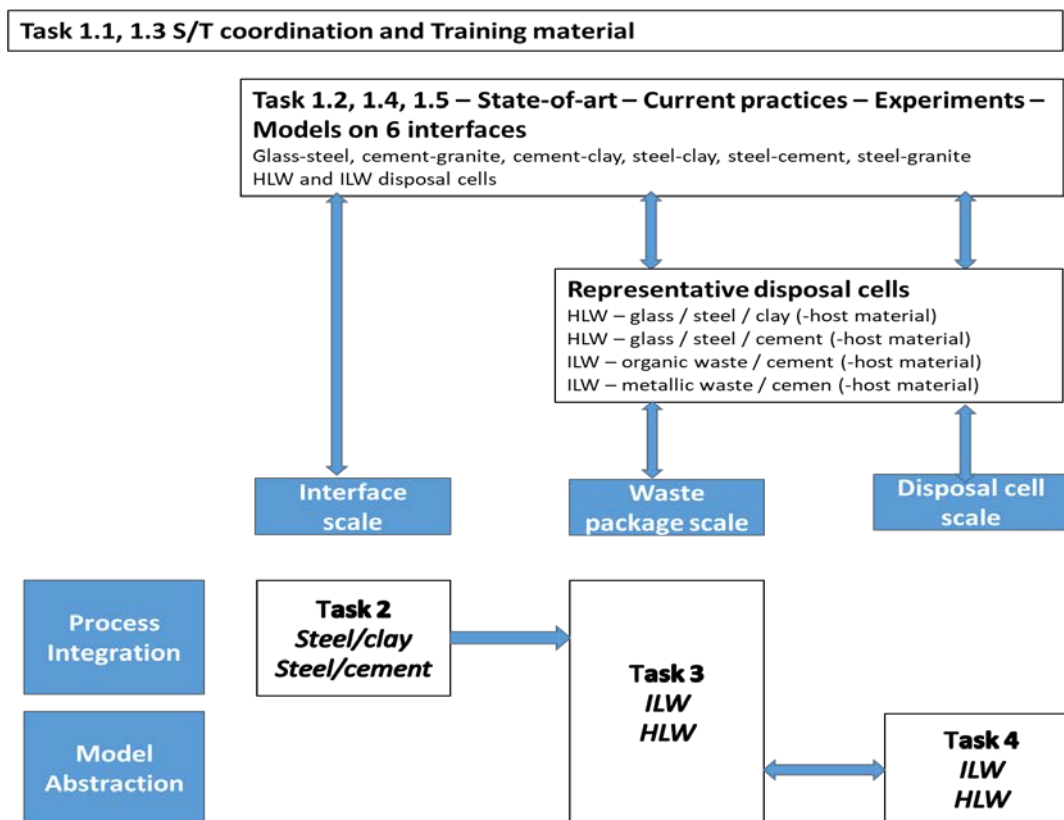


Figure 1-1 – Overall scope of the project, together with the link to (sub)task and information exchange between tasks.



**EURAD** Deliverable D2.10 – HLW: Report describing the selected experiments and the existing / expected experimental results

These systems allow for studying the different interfaces expected in HLW disposal cells with vitrified waste, metallic components (containers and possible overpack and liner), presence of cementitious material (e.g. a cement-base grout in the French concept and a cementitious overpack in the Belgian one) and near-field host rock. Although the experimental systems are set-up within a specific disposal concept, the sequence of interfaces represents a broad range of possibilities relevant for many concepts.

HL vitrified waste will be altered in contact with the host rock groundwater having drilled through the cementitious material (if present) and the corrosion products of metallic components. The glass alteration rate highly depends on the chemistry (pH, concentrations in silica, calcium and magnesium in solution) of the aqueous phase, and on the nature of corrosion products formed during the corrosion of the overpack before its failure.

Deliverable D 2.10 provides

- a detailed overview of selected existing experimental data with details on the used materials and methods,
- identify further information that will be available during ACED,
- point out any other information that could be useful for partners involved in Tasks 2, 3 and 4.

## 2. Experiment 1: Glass/Steel/Clay system, 50°C

Glass/Steel/Clay	
Partner:	CEA
Experiment id:	Glass/steel/clay 50°C 2.5 and 6 yr
Contact person:	S. Gin (stephane.gin@cea.fr)

### Description of the experiment - Background

In EURAD ACED, we will focus on two similar integrated mockups allowing us to decipher the interactions between SON68 glass, steel (corroded and pristine) and Callovo-Oxfordian claystone. One experiment is still running and will be stopped after approximately 6 years. Besides, a similar mockup was stopped after 2.5 y and was thoroughly investigated within the course of a previous PhD work (Carriere, 2017). It is planned to use the data available from this 2.5 y old experiment for modeling and perform various analyses on the still running experiment that will be dismantled within ACED after 6 years. The data displayed here come from the 2.5-year-old experiment.

The principle of the mockup is illustrated in Figure 2-1.

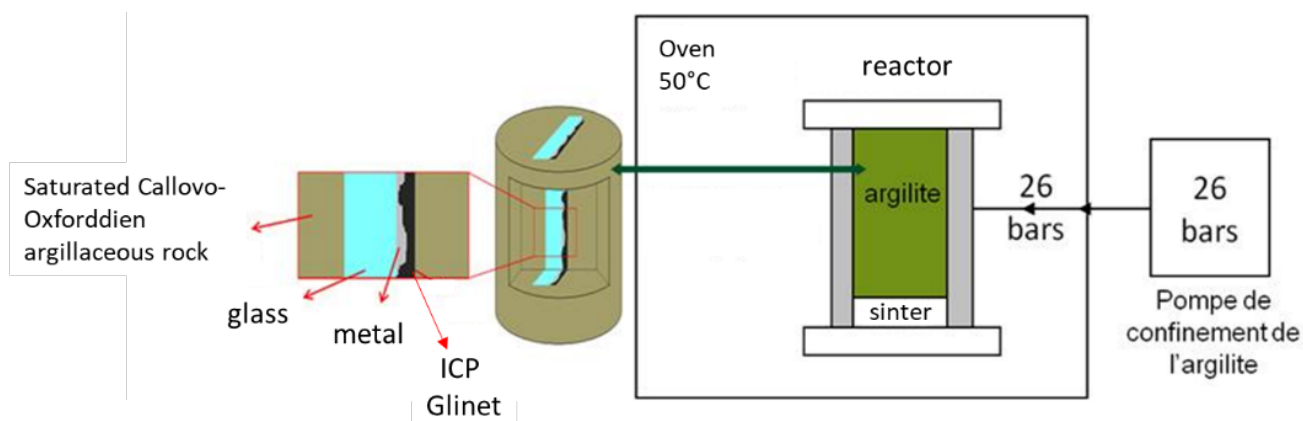


Figure 2-1 – Experimental setup

Briefly, a cylindrical core ( diameter ~5 cm, length ~8 cm) of Callovo-Oxfordian (COx) claystone sampled at the Meuse/Haute-Marne URL was cut in two half-cylinders and machined in order to place in the middle a coupon of SON68 glass doped with <sup>29</sup>Si and <sup>57</sup>Fe pressed against a piece of iron prepared from a 450 yr old nail recovered from the Glinet site (Normandy) and containing both corrosion products and pristine iron. Once rebuilt the system was placed in a membrane and was resaturated with synthetic COx ground water. The system then aged in an oven at 50°C for 2.5 years. No sample was taken during the course of the experiment. At the end, the whole system was frozen, lyophilized and embedded in epoxy. Cross sections were prepared and characterized by various analytical techniques: optical microscopy, Raman spectroscopy, SEM, ToF-SIMS, TEM, and STXM. The characterization mostly focused on glass alteration and iron corrosion. Little was done on mineralogical transformations within the clay and on the fate of major elements such as Si, Al, Fe. Moreover, no information on solution chemistry were obtained and no modeling work was performed.

The characterization of the 6-year old experiment will give us complementary data, as well as a second interaction time that is of primary importance for comparison to geochemical simulations. Note that the interactions taken place at the scale of these experiments will be modelled within the frame of the PhD work started in October 2019. This work will then focus on both characterization and modeling.

<b>Materials involved : chemical composition</b>																									
Host rock: Callovo-Oxfordian clay																									
Buffer material: no																									
Canister: iron and iron corrosion products (mainly siderite)																									
Waste: SON68 glass doped with <sup>29</sup> Si and <sup>57</sup> Fe																									
Leaching solution: initial composition																									
<i>Table 2-1 – Initial composition of the leaching solution</i>																									
	<table border="1"> <thead> <tr> <th></th> <th>Na</th> <th>K</th> <th>Ca</th> <th>Mg</th> <th>Sr</th> <th>Si</th> <th>Cl</th> <th>SO<sub>4</sub></th> <th>HCO<sub>3</sub></th> <th>Eh</th> <th>pH</th> </tr> </thead> <tbody> <tr> <td>mg/L</td> <td>966</td> <td>39,1</td> <td>397</td> <td>99,6</td> <td>17,5</td> <td>9,8</td> <td>1453</td> <td>1345</td> <td>232</td> <td>-0,14 V/ENH</td> <td>6,86</td> </tr> </tbody> </table>		Na	K	Ca	Mg	Sr	Si	Cl	SO <sub>4</sub>	HCO <sub>3</sub>	Eh	pH	mg/L	966	39,1	397	99,6	17,5	9,8	1453	1345	232	-0,14 V/ENH	6,86
	Na	K	Ca	Mg	Sr	Si	Cl	SO <sub>4</sub>	HCO <sub>3</sub>	Eh	pH														
mg/L	966	39,1	397	99,6	17,5	9,8	1453	1345	232	-0,14 V/ENH	6,86														
Potential further information of interest but not yet available: pore water composition																									
<b>Schedule</b>																									
Starting point	Jan 2014																								
Dates of sampling	No sampling																								
End point	June 2016 and ~Nov 2019																								
Samples already available	Cross sections from the 2.5 year old experiment																								
Samples that will be available during the EURAD project	Many samples from the two mockups																								
<b>Solid or interface characterization</b>																									
Method(s):	<input checked="" type="checkbox"/> SEM <input type="checkbox"/> XRD <input type="checkbox"/> Other: TEM and Tof-SIMS																								
Operating conditions:																									
Uncertainties associated to the different techniques																									
<b>Results already available</b>																									
<p><i>Figure 2-2 to 2-5</i> give some examples of data obtained from the 2.5 year experiment.</p> <p><i>Figure 2-2</i> presents the region of interest, i.e. the doped glass/iron interface. The right side is characterized by a glass alteration layer (GAL) which has been separated from the pristine glass (PG) and extends to the metal, and visible iron corrosion products (ICP).</p>																									

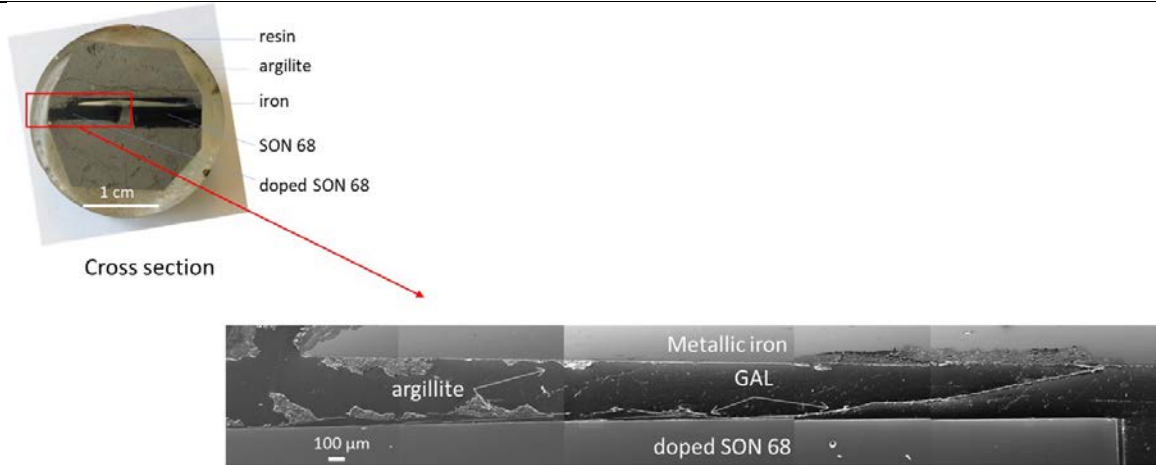


Figure 2-2 – Global view of the glass/steel interface. GAL stands for glass altered layer.

Along the glass, the GAL thickness does not vary and measures  $5 \mu\text{m} \pm 1$ . The main elements contained in GAL are iron, silicon, oxygen, aluminum and zirconium (Figure 2-3). The GAL is Na free, due to glass hydration and inter-diffusion mechanisms. Si/Zr ratio decreases from the PG (close to 10) to the GAL (4.4), suggesting glass hydrolysis. However, the GAL is enriched in iron, as the Fe/Si ratios are equal to 0.1 and 2 in PG and GAL respectively.

### Glass alteration layer composition

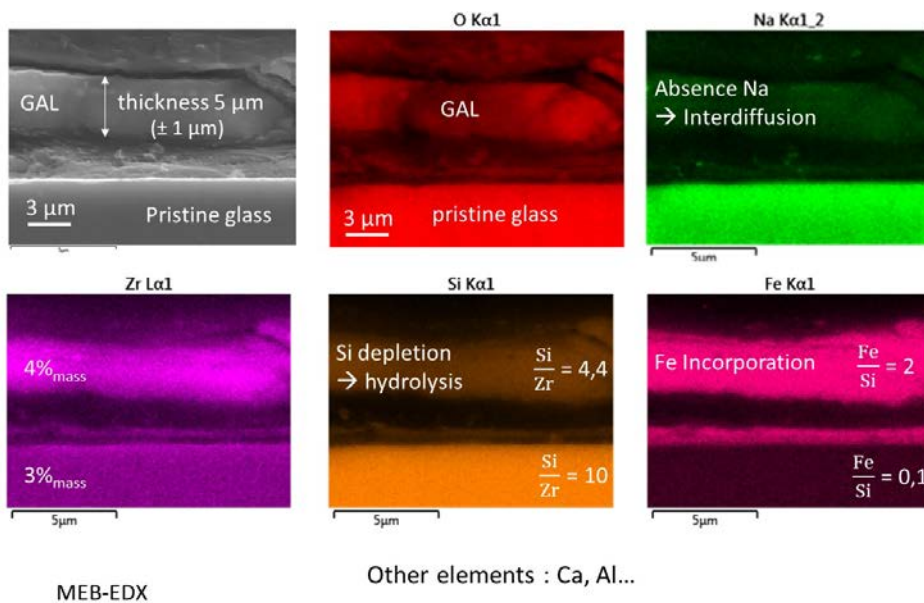


Figure 2-3 – Glass alteration layer determined by SEM-EDX

As the SON68 glass was initially doped in  $^{29}\text{Si}$  and  $^{57}\text{Fe}$ , ToF-SIMS mapping (in positive polarity) was performed in PG and GAL to follow the migration of these 2 elements during glass alteration, and specify Si and Fe origin. As the GAL contained only 20% of  $^{29}\text{Si}^+$ , against 52% expected in PG, the Si constituting the GAL comes from glass alteration (about one third) and COx water solution (two third) (Figure 2-4).

### Si and Fe origin (ToF SIMS measurments)

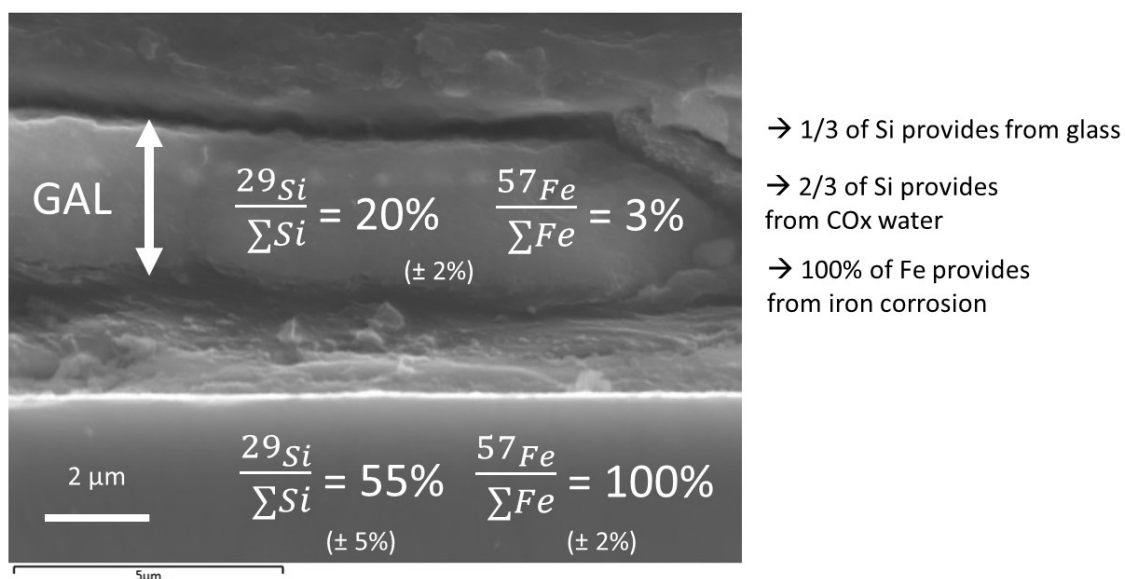


Figure 2-4 – Si and Fe behavior based on ToF-SIMS mapping

TEM observations in GAL evidence presence of crystallized sheets, mainly composed of Si, Fe, O and Al. HRTEM reveals characteristic sheets of clays, with reticular distances of  $10.4 \text{ \AA} \pm 0.6$  between the sheets, corresponding to  $d_{001}$  distance (Figure 2-5). This value is compatible with partially dehydrated smectites.

### Iron silicate identification in GAL at nanometer scale

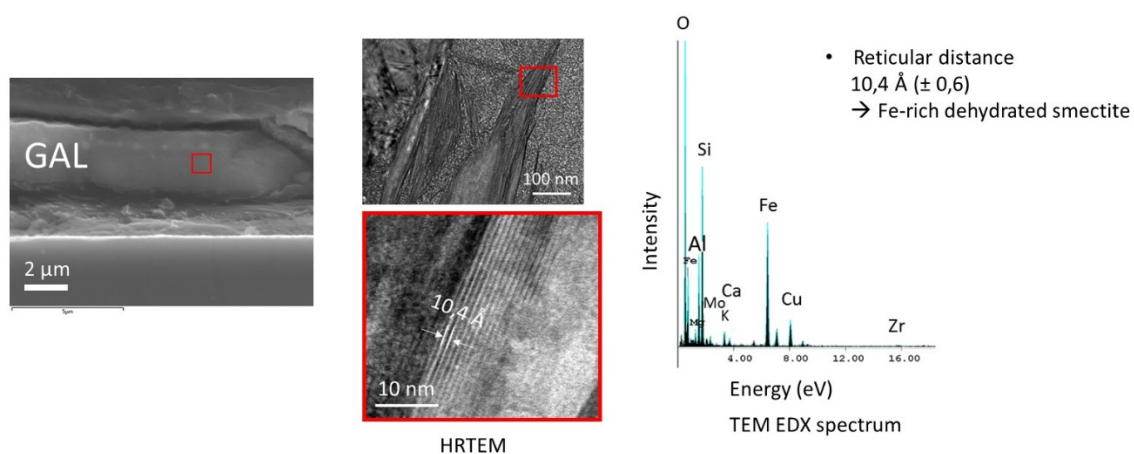


Figure 2-5 – Secondary phases identified by TEM

#### Analysis of leaching solution

Method(s):

Operating conditions:

#### Results already available:

No solution analyses were performed on the 2.5 year old experiment. An attempt will be made with the 6-year old experiment but recovering the pore water is not easy.

### Other tests and characterizations

As explained above, new data will be obtained from the 6 year old experiment within EURAD ACED. In particular, we will try to provide:

- The pore water composition
- The composition and nature of alteration products formed on the glass surface, on the iron coupon and within the clay.
- The location of the chemical fronts for some key elements such as Si, Fe, Al, Mg

### Interfaces with Task 2 and Task 4

Discussion on modeling will start at the same time as that on mockup dismantling. It is envisioned to design parametric tests to constrain the model.

### 3. Experiment 2: Glass/Steel/Cement-bentonite/Clay system, 70°C

Glass/Steel/Cement-bentonite/Clay	
Partner:	EDF / Andra
Experiment id:	EDF / Andra experiment
Contact person:	Dr. Florent Tocino (florent.tocino@edf.fr)
Description of the experiment - Background	
<p>In order to reduce any chemical disturbances, experiments are carried out in watertight reactors in stainless steel (<i>Figure 3-1</i>).</p>  <p><i>Figure 3-1 – Stainless steel reactors.</i></p> <p>Samples are placed in the clay coming directly from the Meuse/Haute-Marne URL. The reactors contain an anoxic leaching solution. The system is static which means the leaching solution is only introduced at the start of the experiment in order to saturate the clay. All the reactors are kept in a stove at 70°C, and the experiments will last up to 3 years (started in May 2018). The experiments are performed with two types of glass, SON 68 glass (R7/T7 surrogate) and AVM V4 representative of the whole French AVM production<sup>1</sup> average behaviour.</p> <p>Each reactor contains 3 types of samples</p> <ul style="list-style-type: none"><li>• The first one is glass powder inside a pierced stainless steel canister: this sample dimensioning has been done in order to observe a decrease in leaching rate during the experiment. In other words, the experiment will capture the transition between initial and residual dissolution rates.</li><li>• The second one is the same but the canister has been coated with magnetite in order to observe the impact of corrosion products.</li><li>• The last one is composed of two glass monoliths squeezed between a stainless steel plate on one side and a steel plate on the other (making a “sandwich” sample) (<i>Figure 3-2</i>).</li></ul> <p>Each setting is tested with and without a cementitious buffer between the different samples and the clay.</p>	

<sup>1</sup> AVM glasses result from vitrification campaigns at the Marcoule vitrification facility (AVM).

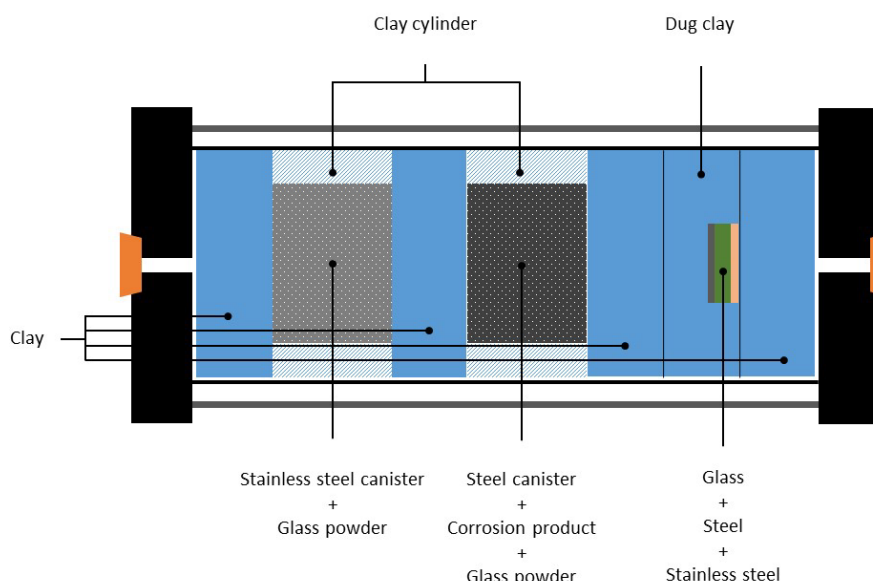


Figure 3-2 – Stainless steel reactor schematic representation (without buffer)

Each reactor is opened after 6, 12, 24 or 36 months, meaning we have a total of 16 configurations (tables 3-1 and 3-2) with 3 samples per reactor. 48 samples will then be characterized by the end of 2021.

Table 3-1 –Configurations tested

Configurations	Names	End (months)			
		6	12	24	36
SON68_cement buffer	S_C	S_C_6	S_C_12	S_C_24	S_C_36
SON68	S	S_6	S_12	S_24	S_36
AVMv4_cement buffer	A_C	A_C_6	A_C_12	A_C_24	A_C_36
AVMv4	A	A_6	A_12	A_24	A_36

Table 3-2 –Schedule

n						n+1						n+2																							
1	2	3	4	5	6	7	8	9	10	11	12	13	14	15	16	17	18	19	20	21	22	23	24	25	26	27	28	29	30	31	32	33	34	35	36
23/05/2018						23/11/2018						23/05/2019						23/05/2020 23/05/2021																	
S_6						S_C_6						S_C_24																							
S_12												S_24																							
A_6						A_C_6						A_C_24																							
A_12												A_24																							
A_C_12						S_C_12																													
						A_C_36																													
						A_36																													
						S_36																													
						S_C_36																													

At the end of the test, reactors are opened. Samples are cut and coated to be kept weeks or even months if needed, they are only polished minutes before characterisation.

SEM observations and EDS analysis are then carried out to determine the alteration layer thickness and its composition.

After more than a year we have successfully opened 7 reactors and analysed 21 samples.

**Materials involved : chemical composition**

Host rock: Host clay (CIGEO site)

Buffer material: Cement-Bentonite grout

Canister: stainless steel, steel

Waste: nuclear glass surrogates (SON 68, AVM V4)

Leaching solution (Table 3-3).

*Table 3-3 –Mass of reagents for 1 kg of solution*

<u>Reagents</u>	<u>Quantities</u>
Al (10 mg/L)	638 µL
CaSO <sub>4</sub> ,7H <sub>2</sub> O	1.6452 g
MgSO <sub>4</sub> ,7H <sub>2</sub> O	1.0120 g
KCl	0.0526 g
NaCl	1.8611 g
Na <sub>2</sub> SO <sub>4</sub>	0.1775 g
SrCl <sub>2</sub> ,6H <sub>2</sub> O	0.0555 g
FeSO <sub>4</sub> ,7H <sub>2</sub> O	0.0141 g
Na <sub>2</sub> SiO <sub>3</sub> ,5H <sub>2</sub> O	0.0746 g
NaHCO <sub>3</sub>	0.4815 g
CaCO <sub>3</sub>	~ 1 g

Potential further information's accessible but not yet available: Specific surface area

**Schedule**

Experiments started in May 2018 and will end most likely in May 2021 (Table 2)

**Solid or interface characterization**

Method(s):	<input checked="" type="checkbox"/> SEM	<input type="checkbox"/> XRD	<input checked="" type="checkbox"/> Other: X-EDS (not available yet)
Operating conditions:	SEM images have been obtained using an FEI SEL QUANTA 650 in environmental mode (P <sub>water</sub> = 140 Pa). Acceleration voltage: 10 kV Working Distance: 10 mm Detector: BSE GAD		
Uncertainties associated to the different techniques			

### Results already available

During the interface characterization the main information we seek is the alteration layer thickness, as it gives us direct information about the dissolution rate. This report will not present all the SEM observations we carried out on the 21 samples we already have. SEM observations showed the presence of an alteration layer on every sample of AVM glass after 6 or 12 months: *Figure 3-3* presents a typical alteration layer observed after 6 months on an AVM glass monolith facing steel. On the contrary, no layer has been found on the SON 68 glass powder samples in any case, only one the monolith samples. Therefore, we are looking forward to opening the next reactors and expect to get some insight on the alteration of this type of glass.

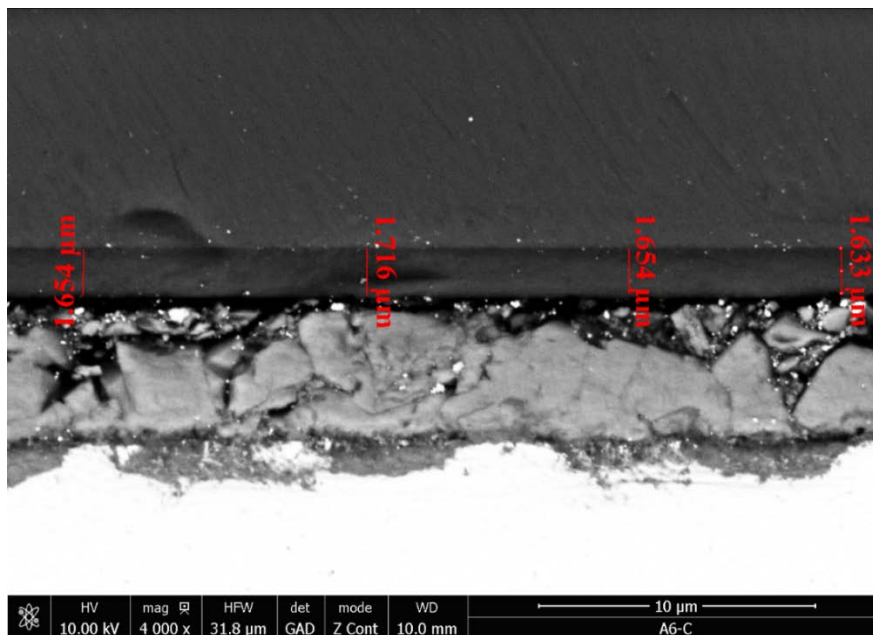


*Figure 3-3 – AVM glass sample monolith facing steel after being dissolved for 6 months*

Regarding the AVM glass we measured the layer thickness at least 20 times for each samples in order to get an average measure and the associated uncertainty. *Figure 3-4* presents all measurements of the alteration layer thickness we obtained on the experiments without cement-based grout.

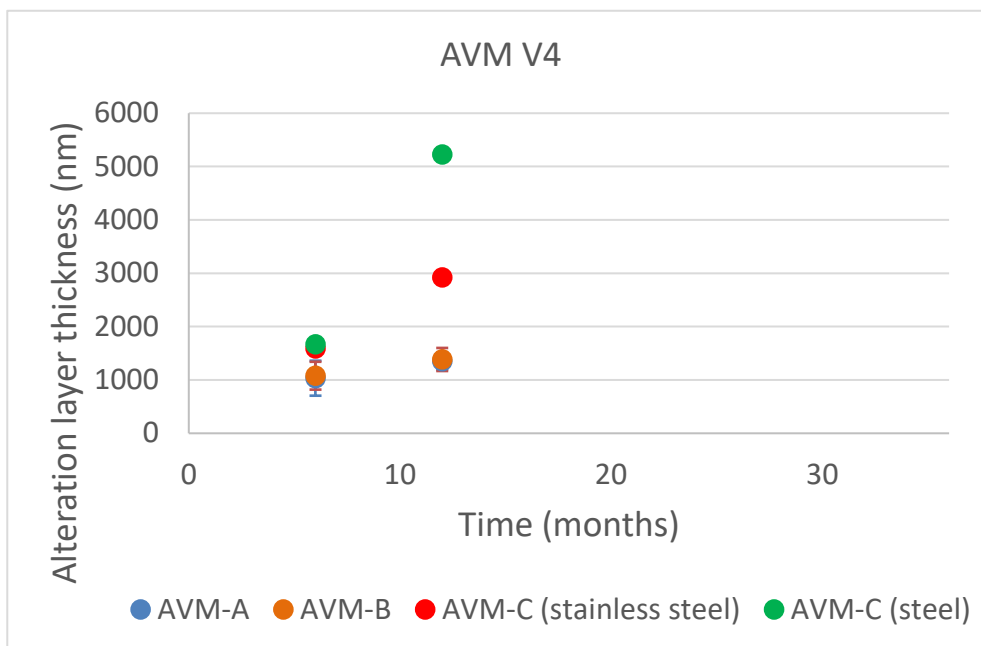


Figure 3-4 – Alteration layer thickness measured on AVM glass after 6 and 12 months. Steel canister (A), steel canister coated with magnetite (B) and “Sandwich” (C).

According to these results the effect of the presence of steel is clear on the last sample (“sandwich” sample) as it increases the dissolution rate (AVM-C experiments in Figure 3-4). This effect is not clearly evidenced on powders, as the difference between sample A and B is not significant.

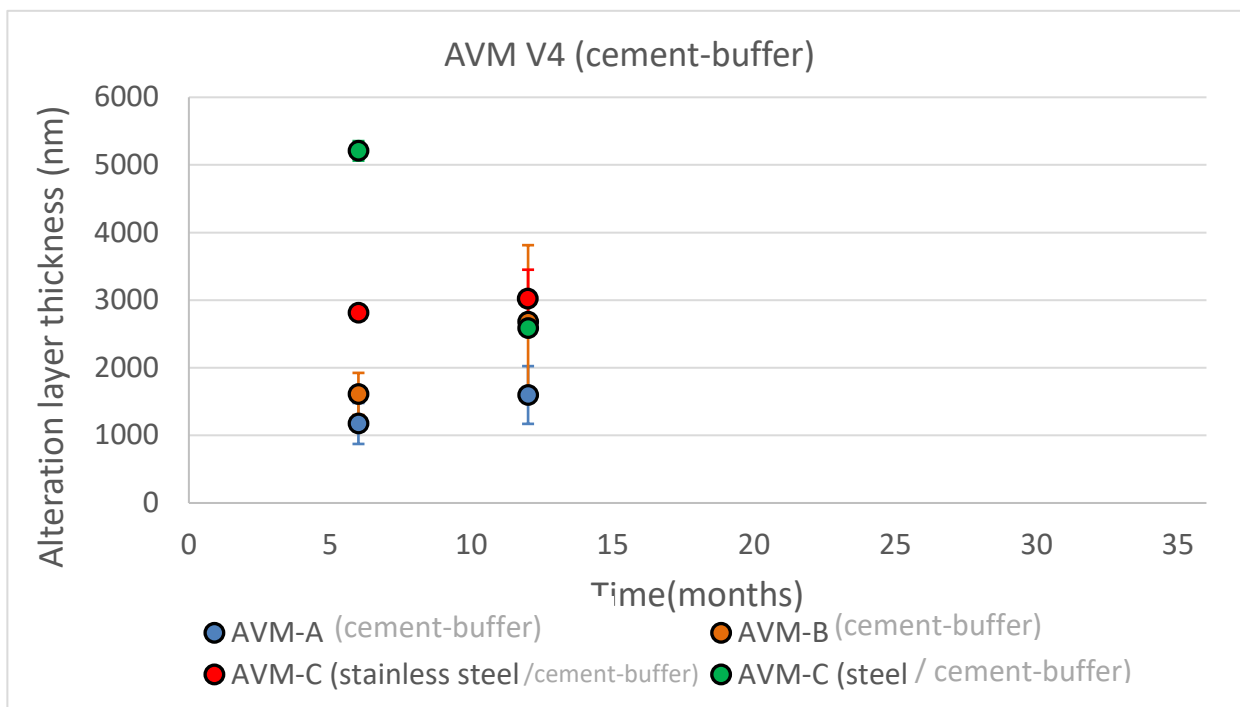


Figure 3-5 – Alteration layer thickness measured on AVM (with buffer) glass after 6 and 12 months

The results on the dissolution of AVM glass sample with the cement-based buffer are presented in Figure 3-5. These results do not show a clear effect of the buffer on the alteration layer thickness and on the dissolution rate as the difference with Figure 3-4 is not significant. Nevertheless, the measure uncertainty increased after 12 months which means the layer thickness is heterogeneous. Also the trend observed on the simulating crack facing steel is not what we expected. Next points (after 24 months) will give us more information about the effect of the buffer.

Analysis of leaching solution	
Method(s):	<input type="checkbox"/> ICP <input type="checkbox"/> <input type="checkbox"/> <input type="checkbox"/>
Operating conditions:	
Results already available:	
Leaching solution cannot be carried out on these experiments because each reactor contains 3 samples. If we were able to recover enough solution (which would be very difficult), the information obtained would be an average concentration not very helpful.	
Other tests and characterizations	
TOF-SIMS characterisations will be carried out on the 3 years lasting experiments, in collaboration with CEA.	
Interfaces with Task 2 and Task 4	

## 4. Experiment 3: Glass/Steel/Cement system, 25°C

<b>Glass/Steel/Cement</b>	
<b>Partner:</b>	SCK•CEN
<b>Experiment id:</b>	Glass/Steel/Cement system, 20 - 25°C
<b>Contact persons:</b>	Karine Ferrand (karine.ferrand@sckcen.be), Karel Lemmens (karel.lemmens@sckcen.be), Sanheng Liu (Sanheng.liu@sckcen.be)

### Description of the experiment - Background

The integrated tests were conducted at room temperature (20 - 25 °C) in stainless steel cells, with a length of 135 mm and an internal diameter of 80 mm, which were filled with hardened ordinary Portland cement paste (water to cement ratio of 0.4) and a layer of glass powder (fraction 125 – 250 µm) separated by a stainless steel filter of 2 mm thick and with a 10 µm porosity. In order to perform sampling of the leaching solution, four holes were drilled in the cement plug (diameter of 6 mm, height of 75 mm) whereas in the glass compartment, a tubular stainless steel filter (110 µm porosity) was placed. The theoretical volume available for sampling was very low, i.e. 2.12 mL in the drilled holes and 3.7 mL in the glass compartment. Based on the amount of glass powder, the density of the glass and the dimensions of the glass compartment, a porosity of 48% for the cell with SM539 and 54% for the cell with SON68 is calculated. This means that the glass compartment, having a total volume of 88 cm<sup>3</sup>, contains 43 mL of water for the cell with SM539 and 48 mL of water for the cell with SON68. A cross section of the cell is presented in *Figure 4-1* and experimental conditions are indicated in Ferrand et al. (2018). Note that there are integrated tests without the stainless steel filter between the cement paste and the glass powder; these tests are also described in Ferrand et al. (2018) but will not be used in ACED.

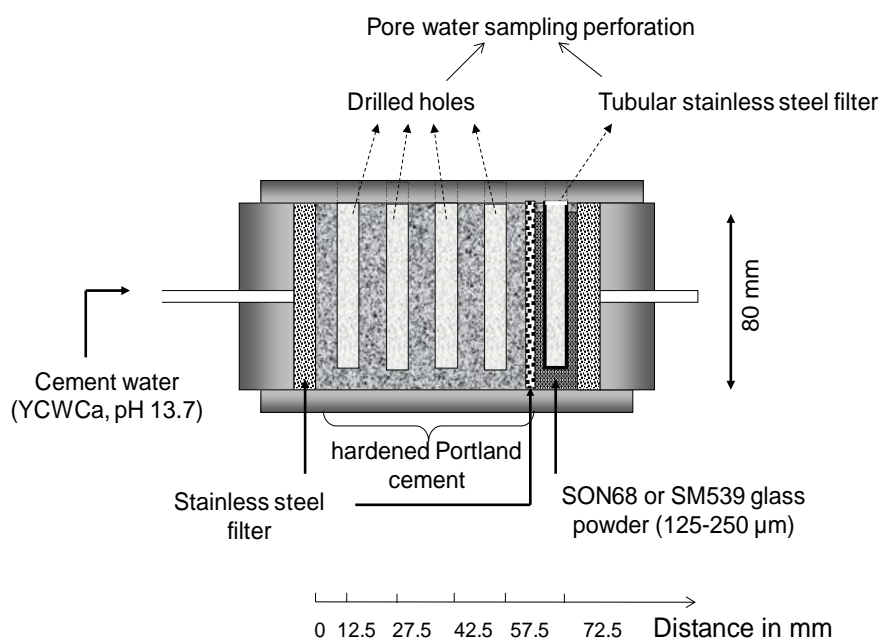


Figure 4-1 – Experimental set-up for the integrated tests.

Table 4-1 –Experimental conditions for the integrated tests (uncertainties are given at  $2\sigma$  (95 % confidence interval)).

Glass	SM539	SON68
Glass (125-250 $\mu\text{m}$ ) weight (g)	$110 \pm 0.005$	$110 \pm 0.005$
Glass layer (mm)	$17.5 \pm 0.02$	$17.5 \pm 0.02$
Glass density ( $\text{g}\cdot\text{cm}^{-3}$ )	$2.45 \pm 0.01$	$2.75 \pm 0.01$
Glass specific surface area ( $\text{m}^2\cdot\text{g}^{-1}$ )*	$0.0310 \pm 0.0002$	$0.0310 \pm 0.0002$
C42.5 R HSR LA CCB cement height (mm)	$64 \pm 0.02$	$64 \pm 0.02$
C42.5 R HSR LA CCB cement weight (g)	$637.6 \pm 1.2$	$648.6 \pm 1.2$

\* the uncertainties given are those reported with the measurements but they are probably very underestimated.

The drilled sampling holes were filled with a synthetic cementitious solution referred to as YCWCa and an increasing Ar pressure from 2 to 15 bar was applied to accelerate the saturation of the cement plug. The holes were regularly checked and refilled when it was necessary. After 1 year, the cell reached a constant weight after addition of a cumulated total volume of YWCa of about 44 mL. When the volume of the glass compartment was filled with the solution, Ar pressure application was stopped to leave the system under static conditions.

After different periods of time (see *Table 4-2*), 1mL of aliquot solution was taken to measure the pH and then diluted with 2 mL of ultrapure water, ultrafiltered (10 000 D), and acidified to be analysed by ICP-AES or ICP-MS and IC.

Note that sampling of the glass compartment was not possible after 586 days in the cell with SON68, because there was enough solution in the tubular filter (nor in the first two cement sampling holes). To allow samplings for longer durations, all sampling holes were refilled with YCWCa for the cell with SON68 and with YCWCa containing 30 mg/L of Si, i.e. the same concentration as one determined after 12 months, for the cell with SM539.

Table 4-2 –Duration in days between the start of the tests (i.e. the percolation date) and the sampling dates.

Glass	Percolation date	Sampling date	Days
SM539	2009-10-28	2010-04-26	180
SM539	2009-10-28	2010-10-28	365
SM539	2009-10-28	2011-04-05	524 <sup>1</sup>
SM539	2009-10-28	2011-10-05	707
SM539	2009-10-28	2012-04-13	898
SON68	2009-08-27	2010-02-24	182
SON68	2009-08-27	2010-09-14	383
SON68	2009-08-27	2011-04-05	586 <sup>2</sup>
SON68	2009-08-27	2011-10-05	769
SON68	2009-08-27	2012-04-13	960

<sup>1</sup> sampling followed by refilling with YCWCa containing 30 mg/L of Si

<sup>2</sup> no sampling in glass compartment, only refilling with YCWCa

After the last sampling, there was an unknown remaining amount of cement water in the glass compartment, so the alteration of the glass particles continued until the cells were dismantled. The tests were dismantled 1530 days after the last sampling. In a first instance, water was removed by applying Ar pressure until a constant weight was reached and then a lyophilisation was done and the whole system was embedded under vacuum with an epoxy resin. Note that during this operation, the resin has not penetrated into the cement paste due to its too low porosity. Afterwards, some sample cores were extracted to perform solid analyses.

Table 4-3 indicates the glass dissolution rates ( $\text{g}\cdot\text{m}^{-2}\cdot\text{d}^{-1}$ ) determined from different leaching tests in YCWCa; it allows drawing the following conclusions:

- The SEM images show that the alteration layer thickness (and the dissolution rate derived from this) of the glass particles in the bulk of the glass compartment was not significantly influenced by the presence or absence of a filter separating the glass from the hardened cement plug. For the glass particles close to the interface with the cement, the effect of the filter on the alteration layer thickness was divergent, but difficult to quantify. The dissolution rate calculated from the boron release, representative for the overall glass dissolution, was 1.5 – 2 time higher without filter than with filter.

- The bulk or overall dissolution rates are similar to the dissolution rates that were measured in another experimental setup, where glass powder was confined between stainless steel filters and leached in YCWCa without cement, but lower than the dissolution rate in cement water with dispersed glass particles without cement or with dispersed cement particles. The dispersion of the glass and cement particles increases the reactive surface area and thus accelerates the interaction.

This shows that the presence of the cement can increase the dissolution rate in YCWCa, but only if there is good contact between glass and cement. When a cement plug is used, the small reactive surface area and transport processes slow down the interaction with the glass.

- The dissolution rate was higher for the glass particles at the interface with the cement plug, where the exchange of solutes with the concrete is the fastest. Further away from the cement, the chemistry of the leaching solution is determined predominantly by the dissolving glass, rather than by the cement. This rate accelerating effect at the interface is larger for SM539 than for SON68. For a complete description of the system, one thus has to specify the dissolution rate at the interface and the dissolution rate further away from the interface. The presence or absence of a filter had little impact on the dissolution rate at the interface.

Table 4-3: Glass dissolution rates in  $\text{g}\cdot\text{m}^{-2}\cdot\text{d}^{-1}$  determined from different leaching tests in YCWCa; the uncertainty at 2 sigma (95% confidence interval is <15%)

Leaching solution: YCWCa	SM539 glass		SON68 glass	
Integrated tests	Filter	No filter	Filter	No filter
From SEM data In the bulk of the glass compartment	<0.003	<0.003	<0.003	<0.003
From SEM data Close to the cement/(filter)/glass interface	<0.05	<0.04	<0.003	<0.005
From [B]	0.0015	0.003	0.001	0.0015
<b>Unconfined glass, 30 °C</b>	0.0065		0.0085	
<b>Confined glass, 30 °C</b>	0.00052		0.00057	

In the integrated tests in which a stainless steel filter was used between the glass and the cement plug, the pozzolanic reaction between Si from the glass and the portlandite in the cement did not lead to a fast dissolution. This was due to slow transport in the cement plug, evidenced by the very small thickness (< 100  $\mu\text{m}$ ) of the altered cement layer, showing chemical and structural changes. The slow transport is expected from the low initial porosity in the cement. Possibly clogging of the pores by the precipitation of secondary phases such as C-S-H, C-A-S-H and zeolites slowed down further the diffusion and hence the pozzolanic reaction, while favouring the build-up of the dissolved matrix constituents, leading to relatively low glass dissolution rates. We found however no direct evidence for such pore clogging. In the tests without filter separating the glass from the cement, there was an increase of the large pores due to the dissolution of portlandite.

**Materials involved : chemical composition**

Host rock: No host rock

Buffer material: ordinary Portland cement paste (C42.5 R HSR LA CCB); its composition is given in Table 4-4. The cement paste was obtained by mixing 1000 g of cement with 400 g of tap water (i.e. W/C = 0.4) directly in the stainless steel cells, removing air bubbles by stirring with a spoon. The cement paste was allowed to harden at room temperature during 20 days.

*Table 4-4 –Average analytical composition in weight % of C42.5 HSR5R LA CCB Portland cement provided by Cibelcor (3 wt% of tricalcium aluminate (C3A) is also reported)*

<b>SiO<sub>2</sub></b>	21.4
<b>Al<sub>2</sub>O<sub>3</sub></b>	3.3
<b>Fe<sub>2</sub>O<sub>3</sub></b>	4.0
<b>CaO</b>	63.3
<b>MgO</b>	2.4
<b>SO<sub>3</sub></b>	2.8
<b>K<sub>2</sub>O</b>	0.57
<b>Na<sub>2</sub>O</b>	0.15
<b>Cl<sup>-</sup></b>	0.03
<b>% Na<sub>2</sub>O eq</b>	0.53
<b>Fire loss</b>	1
<b>Insoluble residues</b>	0.1

Canister: Stainless Steel filter (316L) from GKN, 10 µm average pore size

Waste: SON68 glass (inactive French borosilicate reference glass) and SM539 HE 540-12 glass (PAMELA Belgian reference glass) were used; their composition is given in Table 4-5.

Table 4-5 –Composition of SON68 and SM539 HE 540-12 glasses in weight %

Oxide	SON68	SM539
SiO <sub>2</sub>	45.48	35.27
B <sub>2</sub> O <sub>3</sub>	14.02	25.57
Na <sub>2</sub> O	9.86	8.77
Al <sub>2</sub> O <sub>3</sub>	4.91	20.23
CaO	4.04	5.04
Li <sub>2</sub> O	1.98	3.49
Fe <sub>2</sub> O <sub>3</sub>	2.91	0.45
TiO <sub>2</sub>	0	0.003
NiO	0.74	0.011
Cr <sub>2</sub> O <sub>3</sub>	0.51	0.033
ZnO	2.50	0
P <sub>2</sub> O <sub>5</sub>	0.28	0
SrO	0.33	0.005
ZrO <sub>2</sub>	2.65	0.046
MoO <sub>3</sub>	1.70	0.017
MgO	0	0.130
MnO <sub>2</sub>	0.72	0.035
CoO	0.12	0
Cs <sub>2</sub> O	1.42	0
BaO	0.60	0
Y <sub>2</sub> O <sub>3</sub>	0.20	0
La <sub>2</sub> O <sub>3</sub>	0.90	0.007

Leaching solution: YCWCa at pH<sub>(25°C)</sub> = 13.7 ± 0.2 is used; its composition is given in Table 4-6.

Table 4-6 –Composition of the Young Cement Water with Ca (YCWCa) in mg/L

Element	Al	Ca	K	Na	Si	SO <sub>4</sub> <sup>2-</sup>	TIC
Synthesised YCWCa	0.10	13.8	12300	3200	4.8	183	89

**Potential further information's accessible but not yet available (e.g porosity)**

Porosity is an important parameter for modelling that has still to be determined. If possible, the identification and quantification of the cement phases might also be relevant. Possible analyses that could be performed in the EURAD project have to be discussed with the other partner laboratories (University of Lorraine and IMT Atlantique).

Schedule	
Starting point Dates of sampling End point Samples already available for Deliverable Samples that will be available during the EURAD project	As the tests were carried out many years ago the samples are already available for the EURAD project. They are reported in detail in Ferrand et al. (2018).
Solid or interface characterization	
Method(s):	<input checked="" type="checkbox"/> SEM <input type="checkbox"/> XRD <input type="checkbox"/> Other:
Operating conditions:	The SEM-EDX analysis was performed on C-coated samples using a MIRA 3 TESCAN microscope equipped with a Schottky type Field Emission Gun. The acceleration voltage and the working distance were fixed to 20 kV and 15 mm, respectively. Semi-quantitative EDX analyses were also carried out on the microscope equipped with a LaB6 source operating at 20 kV with a Gatan CCD camera and an EDAX Genesis detector.
Uncertainties associated to the different techniques	For EDX analysis, detection limits are from 0.2% up to 5% depending on the elements, the matrix and the interferences.
Results already available	
<p>SEM analysis reveals that SM539 glass particles close to the stainless steel filter are more altered until a distance of around 800-900 <math>\mu\text{m}</math> from the filter/glass interface. As shown in <i>Figure 4-2</i>, some glass grains present a multi-layer of about 20 <math>\mu\text{m}</math> thick. EDX analysis shows that Al, Si and Ca contents are similar to those in the pristine glass, whereas Na is slightly depleted. Potassium from the leaching solution is strongly retained in the multi-layer. The layers have different densities and compositions, with higher element contents in the outer layer. The concentration gradient is however less significant for Na. Other alteration profiles, i.e. hemispherical alteration layers with a radius up to 40 <math>\mu\text{m}</math> or pits due to the total dissolution of the alteration layers are observed in the whole glass compartment.</p>	
	
<p><i>Figure 4-2 – SEM micrograph of lamellar layers observed on SM539 glass particles close to the filter.</i></p>	
<p>The observation of the cement paste shows that its microstructure and chemical composition are changed on a few hundred micrometers, i.e. on 200-300 <math>\mu\text{m}</math> for SM539 glass (<i>Figure 4-3</i>) and 100-200 <math>\mu\text{m}</math> for SON68 glass. These thicknesses are enriched in K and Na but not in Al.</p>	

Close to the stainless steel filter the porosity is higher in the first 60  $\mu\text{m}$ . Such an increase of the porosity was less visible for SON68 due to the sample preparation, as the cement plug was broken in different pieces during dismantling.

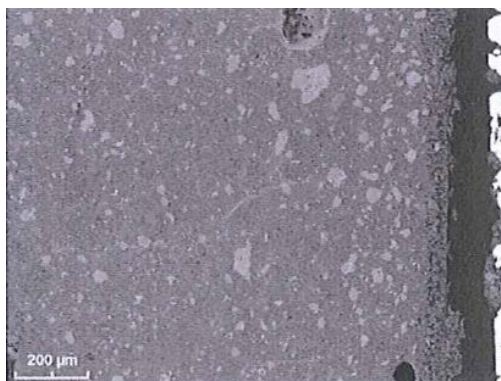


Figure 4-3 – SEM micrograph of the cement plug close to the stainless steel filter in the test with SM539 glass. The filter is situated at the right hand side of the micrograph.

The EDX analysis performed at the cement/filter interface suggests the formation of C-S-H with a low Ca/Si ratio of 0.6 for SON68 glass, and the formation of C-A-S-H with Ca/Si and Al/Si ratios of 0.7 and 3.2 for SM539 glass, both phases incorporating high quantities of K and Na. In the cell with SM539, some pre-existing cracks (not induced by the dismantling) were also visible; they are clogged by precipitation of secondary phases. EDX analysis indicates that these phases are C-S-H with a Ca/Si ratio of about 1 containing alkalis, and a small amount of Al.

As shown in Figure 4-4, air bubbles initially present in the cement paste are filled with ettringite and portlandite and non-spherical holes surrounded by iron are also visible.

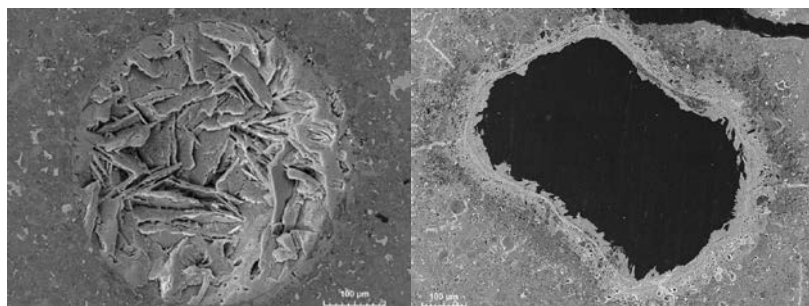


Figure 4-4 – SEM micrographs of a spherical hole filled with ettringite and portlandite, and of a non-spherical hole in the cement plug.

Regardless of the type of glass, the analyses by SEM-EDX of the stainless steel filter show that secondary phases precipitate inside its pores (Figure 4-5). The phases detected in the filter pores close to the glass powder contain a high amount of K, and present a Ca/Si ratio lower than 0.1 and Al/Si ratio of 2.2-2.7. For the Al-rich glass SM539, the pores close to the cement plug are filled with the same phase, but EDX reveals that it incorporates more Ca (Ca/Si= 0.4). For SON68 glass, the phase precipitated in the filter pores close to the cement plug has a Ca/Si of 0.7 indicating the formation of C-S-H phase, containing mainly alkalis and a small amount of Al.

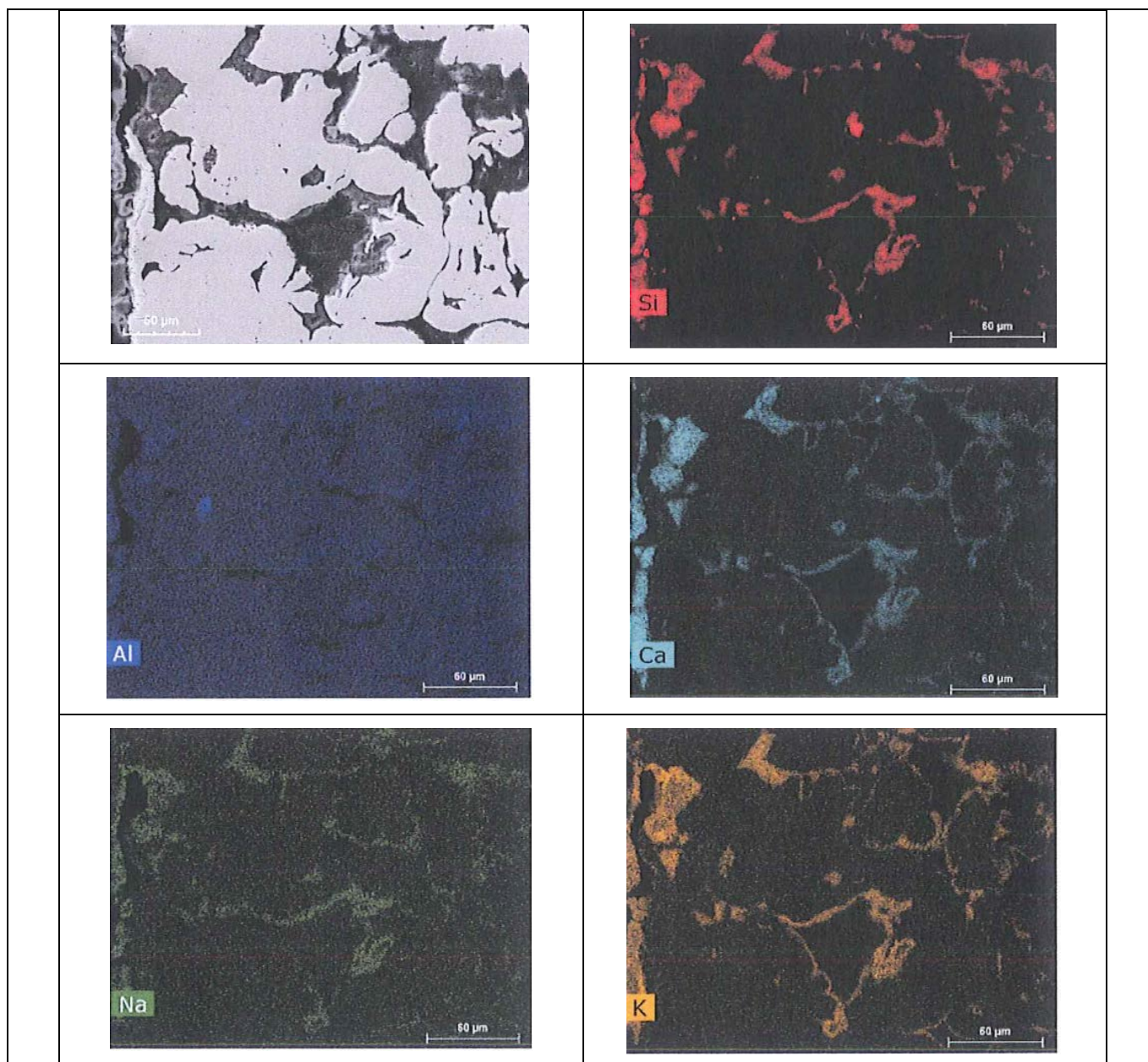


Figure 4-5 – SEM micrograph and EDX elemental mappings of the stainless steel filter close to the cement plug in the test with SON68 glass.

#### Analysis of leaching solution

Method(s):

ICP

IC

Operating conditions:

Samples were diluted with either 5% HCl / 1% HNO<sub>3</sub> or 2 % HNO<sub>3</sub> to determine their chemical composition by ICP-AES using the ThermoScientific Iris Intrepid II dual view apparatus or by ICP-MS using the ThermoScientific Xseries2 apparatus. To perform ionic chromatography, the ThermoScientific Dionex DX600 apparatus was used. For both analytical techniques ICP and IC, the uncertainty at 2 sigma (95% confidence interval) was 10%.

### Results already available:

pH<sub>(25 °C)</sub> appears to be quite constant in the cement plug, i.e. from 12.5 at 52.5 mm, whereas a slightly lower pH is observed in the glass compartment at 72.5 mm, supposedly due to the release of boric and silicic acid from the glass.

The boron concentration measured in the boreholes of the cement paste is very low and constant around 3-9 mg/L, whereas it increases strongly in the glass compartment: up to 1650 mg/L for SON68 glass and up to 3600 mg/L for SM539 glass.

For SON68 glass, high increasing silicon concentrations are measured in the glass compartment, reaching a value of 4193 mg/L after 960 days but probably increasing further afterwards, suggesting that the silicon concentration in solution is not (yet) limited by solubility. For SM539 glass, silicon concentration first increases up 484 mg/L, and then decreases to 288 mg/L, indicating Si incorporation into secondary phases.

The Al concentration in the glass compartment first peaks and then decreases: maximum concentrations of 108 and 11 mg/L are measured for SON68 and SM539 glasses, respectively.

A low Ca concentration of 1 – 5 mg/L is measured in the glass compartment whereas in the cement plug, Ca concentrations are quite constant around 60 mg/L.

The Na concentration increases in the glass compartment whereas it is rather constant in the cement plug, i.e. close to the initial value of 3200 mg/L in YCWCa. In contrast, the evolution of the K concentration shows a slight decrease in the glass compartment as well as in the cement borehole close to the glass.

### Other tests and characterizations

Also integrated tests in which glass powder was placed directly in contact with the cement plug were also carried out (reported in Ferrand et al., 2018). Like for the cells with a stainless steel filters, the cells were dismantled and characterised by SEM-EDX analysis.  $\mu$ -XRD analysis was tried on the SM539 glass/cement sample but did not allow the identification of crystalline phases at the glass/cement interface different from those present further in the cement plug.

Preliminary tests were done using LIBS analysis and allowed estimating Li and B diffusion coefficients in the cement plug.

### Interfaces with Task 2 and Task 4

For modelling the interaction between glass/cement, one-dimensional continuum reactive transport model is preferred, such as Marty et al. (2015). Two-dimensional model can also be used if it is necessary. Since alteration layers at the interface of glass/cement are usually very thin (a few hundred  $\mu$ m), in the model the grid size at the interface should be fine enough to capture the features observed at the interface. One potential issue of such a fine grid will be the long computational time. However, tests with a grid size of 25  $\mu$ m have been tried out and it was found that it is still manageable.

For the cement model, the volume fraction of each hydration product and porosity can be obtained either through a hydration model such as the model of Parrot and Killoh (1984) or using empirical relationships found from classic cement literature, such as Taylor (1997). For example, for a given water to cement ratio (W/C) and hydration degree  $\alpha$ , the capillary and gel porosity can be obtained from the following two equations ([http://iti.northwestern.edu/cement/monograph/Monograph5\\_6\\_1.html](http://iti.northwestern.edu/cement/monograph/Monograph5_6_1.html)).

$$v_{cap} = \frac{w/c - 0.38\alpha}{(0.32 + w/c)} \frac{\text{cm}^3}{\text{cm}^3 \text{ paste}}$$

$$v_{gel} = \frac{0.21\alpha}{(0.32 + w/c)} \frac{\text{cm}^3}{\text{cm}^3 \text{ paste}}$$

For the calculation of effective or pore diffusion coefficient, the total porosity should be used in Archie's law type relationships.

The glass compartment in *Figure 4-1* is preferably modelled as one grid cell, i.e., assuming uniform concentrations of all the elements in this compartment. This should also be the boundary condition in the model. Elements released from the glass diffuse into cement (to the left side in *Figure 4-1*). Note that elemental concentrations in the glass compartment change with the dissolution of the glass, so the boundary condition should be a changing-concentration boundary condition in the model. For the choice of glass dissolution models, simple models are preferred, however, in the end the modelled concentrations should be in agreement with the measured concentrations in the glass compartment. Alkalis and boron sorption onto cement can also be important, the model should therefore also include such processes.

## 5. Concluding remarks

This deliverable intends to give a first overview of information already available on existing or currently running experiments that will be studied in subtask 3.1.

The different systems are consistent with both the interfaces studied in Task 2 and the different existing HLW concepts. The experimental program defined in subtask 3.1 will allow getting information about the chemical evolution at glass/steel/buffer interfaces, mainly the nature of newly formed phases, the glass alteration rate and the corrosion rate, according to the temperature, and the nature of buffer (clay or cement).

A major goal of ACED is to evaluate how to pass information from relatively isolated small-scale processes investigated on interface scale to more complex systems at waste package scale and further to full disposal cell scale. Numerical modelling of the coupling between chemistry, transport processes and material alterations will be a major effort. The modelling work of a HLW waste package and disposal cell will be shared between subtask 3.2 and Task 4.

The subtask 3.2 focuses on modelling the selected reference experiments studied in subtask 3.1 and the evolution of vitrified waste consisting of a glass core encapsulated in an iron/steel canister and in contact with a cement or cement/clay backfill. Experimental data from the different systems studied in task 3.1 and combined with the experiments performed in Task 2 dedicated to steel/clay and steel/cement interface will help to constrain the waste package models scale models performed in task 3.2.

The task 4 will look at the scale of a disposal cell simulating the interactions of the waste packages with each other and with the immediate surrounding near field environment and the host rock. For HLW, this approach may also be focused on transient conditions (thermal and hydraulic transients), the representation of interfaces, and heterogeneities (e.g. gaps) at interfaces in modelling exercises.

The different modelling approach will begin with the experimental data already available at the beginning of ACED and presented in this deliverable. Further experimental data acquired during ACED will allow us to complete/update gradually these input data sets.

## 6. References

ANDRA “Safety Options Report - Operating Part (DoS-Expl)” (2016).

CARRIERE C. “*Influence de la corrosion du fer sur les processus d’altération du verre : approche analytique multi-échelle*”; Thèse de l’Université Pierre et Marie Curie (2017).

FERRAND K., LIU S., and LEMMENS K. “*Integrated leach tests with simulated HLW glass in contact with ordinary Portland cement paste*”; SCK-CEN Report ER-0431; Mol (Belgium); (2018).

MARTY N.C.M., BILSTEIN O., BLANC P., CLARET, F., COCHEPIN, B., GAUCHER E.C., JACQUES D., LARTIGUE J.-E., LIU S., MAYER K.U., MEEUSSEN J.C.L., MUNIER, I., POINTEAU I., SU D., and STEEFEL C.I.; “*Benchmarks for multicomponent reactive transport across a cement/clay interface*”; Comput. Geosci. 19; pp. 635-653; (2015).

NEEFT E., WEETJENS E., VOKAL, A., LEIVO M., COCHEPIN B., MARTIN, C., MUNIER, I., DEISSMANN G., MONTAYA V., POSKAS P., GRIGALIUNIENE D., NARKUNIENE A., GARCIA E., SAMPER J., MONTENEGRO L. and MON A. “*Treatment of chemical evolution in National Programmes*”; D 2.4 of the HORIZON 2020 project EURAD. , EC Grant agreement no: 847593; (2020).

PARROT L.J. and KILLOH D.C.; “*Prediction of cement hydration*”; Br. Ceram. Proc. 35; pp. 41-53; (1984).

TAYLOR H.F.W; “*Cement Chemistry*”; Thomas Telford; (1997).